Swi6/HP1 binding to RNA-DNA hybrids initiates heterochromatin assembly

Jagmohan Singh (jsjagsingh@gmail.com)
Institute of Microbial Technology https://orcid.org/0000-0003-2775-1245

Jyotsna Kumar
Institute of Microbial Technology

Swati Haldar
Institute of Microbial Technology

Neelima Gupta
Institute of Microbial Technology

Viney Kumar
Institute of Microbial Technology

Manisha Thakur
Institute of Microbial Technology

Keerthivasan Chandradoss
Indian Institute of Science Education and Research Mohali

Debarghya Ghose
Institute of Microbial Technology

Dipak Dutta
Institute of Microbial Technology

Kuljeet Sandhu
Indian Institute of Science, Education and Research

Article

Keywords:

Posted Date: September 14th, 2020

DOI: https://doi.org/10.21203/rs.3.rs-64732/v1

Abstract

Heterochromatin formation in fission yeast and metazoans involves di/trimethylation of histone H3 at lysine 9 position (me2/me3-K9-H3) by the histone methyltransferase (HMT) Suv39/Clr4, followed by binding of Swi6/HP1 to me2/me3-K9-H3 via its chromodomain[1]. Subsequent self-association of Swi6/HP1 on adjacent nucleosomes leads to folded heterochromatin structure[1-3]. An alternate model suggests a concerted participation of Clr4 and Swi6/HP1[2,3]. HP1 binding to RNA has been invoked for heterochromatin silencing in metazoans[4,5]. Swi6/HP1 also binds and channels RNA to exosome pathway in fission yeast[6]. Recruitment of Swi6/HP1 to centromere is also dependent on the RNAi pathway[7]. Here we show that Swi6/HP1 exhibits binding to RNAs, ranging from promiscuous, low-affinity binding to mRNAs, to moderate-affinity binding to the RNAi-generated siRNAs corresponding to the repeats present in heterochromatin regions[7], to high affinity binding to the RNA-DNA hybrids cognate to the repeats. Together with sensitivity of Swi6 localization and silencing to RNaseH, our results suggest a dynamic distribution of Swi6/HP1 among the heterochromatin and euchromatic transcripts and binding to RNA-DNA hybrid as an RNAi-dependent and Me2/me3-K9-H3-independent mechanism of recruitment, leading to heterochromatin formation and silencing.

Main Text

Eukaryotic chromatin is organized into expressed/euchromatic and repressed/heterochromatic regions through a gamut of distinct post-translational histone modifications[8]. In fission yeast (*Schizosaccharomyces pombe*) and metazoans, freshly assembled chromatin contains histone H3 acetylated at K9 and K14 residues[9]. At heterochromatin regions, the H3-acetyl groups are removed by the deacetylases, Clr3, Clr6 and Sir2, followed by di- and tri-methylation of K9 by Suv39/Clr4[9]. Heterochromatin protein Swi6/HP1 binds to Me2/Me3-H3-K9 through its chromodomain[10]. Subsequent self-association of HP1/Swi6 through its chromoshadow domain results in a folded, transcriptionally inactive heterochromatin[11]. The RNAi pathway is also involved in heterochromatin assembly as the *rnai* mutants show impaired H3K9 dimethylation and Swi6 recruitment at the mating type and centromere loci[7].

According to the current model, the double-stranded (ds) RNAs formed by bidirectional transcription from the *dg-dh* repeat regions are cleaved by Dcr1 to produce the ds siRNAs. These siRNAs are bound to the ARC (Argonaute small interfering RNA chaperone) complex, which contains the endoribonuclease 1 (Ago1), Arb1 and Arb2 subunits[12]. After the passenger strand release, the guide strand is transferred to the chromatin-bound complex, called RNA-induced transcriptional silencing (RITS) complex[13], which consists of Ago1, Chp1- a chromodomain protein and Tas3. The binding of Chp1 to Me2/Me3-K9-H3 tethers the RITS complex to heterochromatin. Subsequently, Rdp1 (RNA-dependent RNA polymerase)[14] generates the double-stranded (ds) RNA by copying the ncRNA strand synthesized by RNA PolII, using the guide strand as a primer. In turn, the ds RNA, is cleaved by Dcr1 to produce the siRNA, thus completing the

amplification cycle[15]. The RNAi link to the formation of Me2/Me3-K9-H3 possibly occurs through Stc1-dependent recruitment of the HMT Clr4-containing CLRC (CLR like Clr4 complex)[16,17].

Earlier studies showed that chromodomains could act as RNA-binding domains[4] and RNA binding by the murine HP1 through its chromo- and hinge domains is required for heterochromatin assembly[5]. However, another study proposed that heterochromatin-transcribed RNA competes with Lys9 methylated H3 for binding to Swi6 and is carried to the exosome[6]

Here, we investigated whether, similar to metazoans, Swi6/HP1 may be recruited by binding to the si RNAs in *S. pombe*. This scenario is consistent with the loss of heterochromatin recruitment of Swi6 as well as siRNA generation in *rnai* mutants[7]. Indeed, the siRNAs found *in vivo* (labeled A-K)[18] or generated *in vitro*[19] were mapped to the *dg* and *dh* repeats that are shared among the outer repeats (*otr*) on all three centromeres[19], the *cenH*[20] region (*mat2-mat3* interval) on *chrII* and the subtelomeric *tlh1* and *tlh2* genes on *chrI* and *chrII*[21] (Fig. 1a,b; Extended Data Fig. 1 and 2; Extended Data Tables 1 and 2).

By pairwise alignment of the siRNA sequences[18,19] (Extended Data Fig. 2) we constructed DNA templates comprising the T7 promoter linked with the *dg-dh* DNA sequences cognate to the siRNA sequences, denoted as B,D,E H and K[18] (Fig. 1b), and I-IX[19], generated by Dicer mediated cleavage of “RevCen” RNA (Extended Data Table 2). The respective single stranded (ss)-siRNAs were generated by using T7 RNA polymerase (Extended Data Fig. 3a, Table 3). Of these, the siRNAs, denoted as ‘D-For’ and ‘E-For’ were radiolabeled and used to study the interaction with Swi6 (Extended Data Fig. 3b;c) by Electrophoretic Mobility Shift Assay (EMSA; Fig. 1c). Binding of Swi6 with the ‘D-For’ RNA was indicated by slow migrating bands I, II and III, representing different complexes (Fig. 1c). The binding was specific, as it was competed out by excess of unlabeled D-For RNA (Fig. 1c). No binding was detecred with the complementary D-Rev RNA (not shown).Other ssRNAs B, E and H (Fig. 1c) and K (not shown) (as well as I-IX; Extended Data Fig. 4a,b) also competed efficiently, suggesting the presence of conserved sequence elements in the ‘A-K’ siRNAs (Fig. 1d). The strength of binding/competition efficiency was in the order: B>D=E>H. A consensus Swi6/HP1-binding sequence obtained by sequence alignment[22] was: G/C.A.G.T/C/A.A.G/T/A.G/C.G/T.G/C/A.T (Extended Data Fig. 5).

The equilibrium binding constant, Kd, for Swi6/HP1 binding to ‘D-For’ RNA was estimated to be 2.15±0.1mM (Fig. 1e)[23]. This binding affinity is ~17.5-fold stronger than that reported for the euchromatic, ‘Cen100’ RNA corresponding to the thymidylate kinase gene (Kd=38mM)[6]. We noted that in the latter study EMSA was done in agarose gel, which can detect weaker binding[6]. Indeed, an EMSA using polyacrylamide gel failed to detect any binding of Swi6 to the ‘Cen100' RNA (Extended Data Fig. 6a) or the 'RevCen” RNA[19] (Extended Data Fig. 6b), the putative heterochromatic si-RNA precursor. Thus, Swi6 shows stronger affinity towards the small RNAs like ‘D-For’ and ‘E-For’ than the euchromatic and heterochromatic RNAs.

RNA-binding by the chromodomain in murine HP1a was influenced by the hinge domain, in particular, by the lysine triplet sequence in the hinge domain[5]. Sequence comparison showed that this lysine triplet is conserved between the murine HP1 and Swi6/HP1 (residues 242-244; Fig. 1f). We found that, like HP1a, both the CD and CD-hinge but not the CSD region of Swi6 exhibit strong binding to the 'E-For' (used interchangeably with D-For because of similar affinity; Fig. 1g; 1h)). Furthermore, similar to HP15a, the siRNA binding is drastically reduced in case of the Swi6$^{3K\rightarrow3A}$ protein (lysine triplet mutated to alanine; Fig. 1d, right panel).

We validated these results *in vivo* using RNA immunoprecipitation (RIP-seq) analysis. The radiolabelled RNA isolated from immunoprecipitates of extracts of cells expressing *GFP-swi6*$^{+}$, but not *GFP-swi6*$^{3K\rightarrow3A}$ or empty vector with anti-GFP antibody was hybridized with blots containing DNA fragments of *dg*, *dh*, *cenH* (*dhk*) but not with a*ct1* (Extended Data Fig. 7b). Visualization of the radiolabelled size-fractionated siRNA by denaturing urea/acrylamide gel electrophoresis indicated a qualitative and quantitative change in siRNAs.in *swi6*$^{3K\rightarrow3A}$ mutant, as compared with *swi6*$^{+}$ (Extended Data Fig. 7c). These results indicate that Swi6^{+} protein binds and protects the *dg-dh* siRNA from degradation but Swi6$^{3K\rightarrow3A}$ does not. RT-PCR analysis revealed the lack of bidirectional transcription in *swi6D* strain as well as the transformed strains (Extended Data Fig. 7d), while *dcr1D* strain showed accumulation of bidirectional transcripts of *dg-dh* repeats, as shown earlier[7](Extended Data Fig. 7d). These results argue against a role of Swi6 and Swi6$^{3K\rightarrow3A}$ in generation of siRNAs.

Further, the size-fractionated small RNAs were subjected to RIP-Seq analysis. We observed no change in the genome wide occupancy of siRNAs bound to Swi6p and Swi6$^{3K\rightarrow3A}$p (Fig. 2a, left panel). However, we did observe a considerable depletion of siRNA corresponding to the *dg* and *dh* repeats in all three centromeres (Fig. 2a,b; p= 0.001; Extended Data Fig. 8a), the *dh* repeats in the *tlh1* and *tlh2* genes[21] (Fig. 2a, b; Extended Data Fig. 8b; p=0.02), and *cenH* region of the *mat* locus (Fig. 2a,b) in the *swi6*$^{3K\rightarrow3A}$ mutant as compared to *swi6*$^{+}$ strain. This is consistent with the report that Swi6 remains bound to sub-telomeric domains in the absence of telomeric repeats[24], implying prominent subtelomeric heterochromatinization by Swi6 and associated siRNAs.

To validate the EMSA results we analyzed the RIP-seq signals in the genomics bins containing the sequence motifs A-K[18]. The analysis clearly showed significantly reduced enrichment of the reported siRNAs[18] bound to Swi6$^{3K\rightarrow3A}$ versus the Swi6^{+} protein (Fig. 2c), confirming that these siRNAs do interact with Swi6 but not Swi6$^{3K\rightarrow3A}$ *in vivo*.

We further analyzed whether the *swi6*$^{3K\rightarrow3A}$ mutation affects the heterochromatin localization of GFP tagged Swi6. As reported earlier[25], ~65% of *swi6*$^{+}$ cells contain 3 spots, ~25% cells two spots and 10% cells one spot GFP-Swi6 (Extended Data Fig. 9a,b). However, in *swi6*$^{3K\rightarrow3A}$ mutant, only ~20% cells each contained one, two or three spots or diffuse appearance (Extended Data Fig 9a,b), consistent with delocalization of Swi6 from heterochromatin and loss of silencing[25]. We performed plate and ChIP assay to assess the effect of the *swi6*$^{3K\rightarrow3A}$ mutation on silencing. Indeed, we observed derepression of the

ade6 reporter at the outer repeat *otr1R* and *ura4* at the inner repeat *imr1L* of *cenI* in *swi6*$^{3K\rightarrow 3A}$ mutant, as indicated by growth of pink colonies on adenine limiting media (Fig. 3a,b) or enhanced growth of cells on plates lacking uracil, respectively (Fig. 3e)[26]. Complementing these results, ChIP assay showed reduced localization of Swi6 and Me2-K9-H3 at the *ade6* (Fig. 3c,d) and Swi6 at the *ura4* reporter, respectively (Fig. 3f,g). Similar loss of silencing at the *his3-telo* locus[27] was indicated by enhanced growth of the *swi6*$^{3K\rightarrow 3A}$ strain on plates lacking histidine (Fig. 3h,i); this as accompanied by reduced localization of mutant Swi6 at the *his3-telo* locus (Fig. 3j,k). The abrogation of silencing of the *mat2*-linked *ura4* reporter in the *swi6*$^{3K\rightarrow 3A}$ mutant, was indicated by lack of restoration of FOA sensitivity in *swi6D* strain by the *swi6*$^{3K\rightarrow 3A}$ gene (Extended DataFig. 9c,d). Furthermore, in the homothallic, efficiently switching background (*h*^{90}), the *swi6*$^{+}$ gene restored efficient switching to the *h*^{90} *swi6D* mutant, as indicated by enhanced iodine staining of the transformants (ref. 27; Methods; Fig. 3e), but the mutant *swi6*$^{3K\rightarrow 3A}$ did not (Extended Data Fig. 9e).

We envisaged that the si-RNA binding by Swi6/HP1 could facilitate its recruitment to the cognate complementary sequences in the genome. This suggested that Swi6^{+} can bind to the siRNAs as RNA-DNA hybrid. Indeed, EMSA experiment confirmed the binding of Swi6 to the 'D-For' RNA-DNA hybrid with very high affinity (Kd=0.17±0.05mM; Fig. 4b), while Swi6$^{3K\rightarrow 3A}$ showed no binding (Fig. 4a).

To confirm the RNA-DNA binding by Swi6/HP1 *in vivo*, we checked the susceptibility of heterochromatin formation to RNaseH, which cleaves the RNA-DNA hybrids. Indeed, overexpression of *rnh1* (RNaseH1) but not *rnh201* (RNaseH2 subunit A) in cells expressing GFP-tagged Swi6 caused delocalization of GFP-Swi6 as visualized by confocal microscopy (Fig. 4c,d; Extended Data Fig. 10). This was accompanied by loss of silencing of the *ade6* reporter at the *otrR* repeat of *cenI* and *mat3* locus, as indicated by growth of pink colonies on adenine limiting medium (Fig. 4e,f,g; Extended Data Fig. 11a,b,c), while ChIP assay showed reduced localization of Swi6 at both loci (Fig. 4h, Extended Data Fig.11d) in cells transformed with *rnh1* but not by empty vector or *rnh201*. Overexpression of *rnh1* also elicited loss of silencing at the *mat2P* locus in a strain containing a stable *mat1M* locus, as indicated by iodine staining assay[27] (See Methods; Extended data Fig. 11e,f,g) and ChIP assay showed loss of Swi6 localization at the *mat2*-linked *ura4* reporter (Extended Data Fig. 11h). These results confirm that localization of Swi6 to the *dg-dh* repeats (and spreading, as in case of *mat2::ura4* and *mat3:: ade6*) is dependent on its binding to RNA-DNA hybrid.

To check whether Swi6/HP1 binds and protects the *dg-dh* repeats existing as RNA-DNA hybrid *in vivo*, we performed the DNA RNA Immunoprecipitation (DRIP) experiment[29] using the monoclonal antibody against RNA-DNA hybrid[30]. Chromatin samples that were immunoprecipitated with the antibody were treated with RNaseH (light grey bars, Extended Data Fig.12a) and the RNaseH-resistant *dh* regions were quantitated by real time PCR. The treatment with RNaseH *in vitro* caused a 2-fold reduction of the *dh* signal in *swi6*$^{3K\rightarrow 3A}$ as compared to the *swi6*$^{+}$ cells and also in *swi6D* cells transformed with the empty vector and *swi6*$^{3K\rightarrow 3A}$, as compared to *swi6*$^{+}$ gene (Fig.12a), supporting a role of Swi6 in binding and protecting the RNA- DNA hybrid.

It was shown earlier that the level of siRNAs originating from the outer repeats of centromere is reduced in *cid14D* mutant, which is defective in polyadenylation of RNAs and their subsequent degradation by the exosome pathway, resulting in accumulation of pre-mRNAs and ribosomal RNAs[31]. Results of real time PCR confirm that the level of Swi6 recruitment to the *dh* repeats is reduced in the *cid14D* mutant (Extended Data Fig. 12b). As the siRNAs' level is reducedin *cid14D* mutant, we speculate that siRNA binding may be the first step in recruitment of Swi6 to the *dg-dh* repeats.

Earlier, the "Cen100" RNA (corresponding to thymidylate kinase gene) was shown to compete with Me2/Me3/-K9-H3 for Swi6 binding[6]. We performed EMSA assay to determine whether the binding of Swi6 to the D-For RNA/DNA hybrid affected its binding to the Me2/Me3-K9-H3 peptide. Surprisingly, we observed a dose-dependent super-shift in the binding pattern of Swi6 in presence of Me2-K9-H3 (Extended Data Fig. 23c, M2) and to a lesser extent with Me3-K9-H3 peptide (Extended Data Fig. 12c, M3) but not with the unmethylated H3 peptide (Extended Data Fig. 12c, M0). Thus, the high affinity binding of Swi6 to the *dg-dh* specific RNA/DNA hybrid facilitates the binding to Me2-K9-H3 rather than competing against it. We got similar results with D For RNA indicating that Swi6 binding with Cen100 is different from D For RN (not shown).

Next we asked whether the loss of binding by Swi6$^{3K\rightarrow3A}$ mutant protein to the siRNAs generated from the *dg-dh* repeats may shift its binding to non-heterochromatic RNAs. We compared the regions with >2-fold increase in siRNA enrichment in mutant with the regions exhibiting >2 fold increase in WT, for the enrichment of Swi6, RNA PolII, Me3-K36-H3, from the ChIP-seq signals and the gene expression values. Indeed, siRNAs bound to the Swi6$^{3K\rightarrow3A}$ protein were mapped to regions that show less association with Swi6^{+} and greater enrichment of RNA PolII and Me3-K36-H3, which is associated with transcription elongtion[32], as well as higher gene expression values, implying the loss of specificity of Swi6$^{3K\rightarrow3A}$ for *dg-dh* siRNAs and a general non-specific shift towards abundantly transcribing regions (Extended Data Fig.13). Interestingly, a similar shift occurs in case of the 'Cen100' RNA (SPAC15E1.04; Extended Data Fig. 14).

Here, we report that Swi6/HP1 displays a hierarchy of binding affinities to RNA and DNA sequences: i) weak affinity to the euchromatic transcripts like Cen100, ii) moderate affinity with sequence specificity towards the ss-siRNAs corresponding to the dg-dh repeats, which is >15- fold stronger than that towards 'Cen100' and iii) strongest binding (over 220-fold) to the *dg-dh* sequences as RNA-DNA hybrid. This property of Swi6/HP1 governs its localization, in a *cis*- acting manner, to the cognate sites in DNA and helps to initiate heterochromatin formation and silencing. This mechanism of Swi6/HP1recruitment is independent of histone methylation but dependent on RNAi pathway. We speculate that the siRNAs bound to Swi6/HP1 may be chaperoned to the *dg-dh* sequences by sequence complementarity. The cognate sites may be unwound due to transcription by RNA PolII and/or Rdp1 and/or association with the RITS complex, which exists as a RNA-DNA heteroduplex and is susceptible to RNaseH1[33,34]. This window of opportunity may allow Swi6 trafficking from the RNA-bound to the RNA-DNA- bound form. The stronger binding may help to lock Swi6 stably to RNA-DNA hybrid rendering it resistant to RNaseH.

Subsequently, the Swi6-bound Clr4 may initiate lysine methylation[2,3], initiating heterochromatin spreading by further binding of Swi6/HP1 to Me2-K9-H3 (Extended Data, Fig. 15). This scenario can explain the apparent discrepancy between the delocalization of Swi6 upon overexpression of RNaseh1 and protection of RNA-DNA hybrids by Swi6. Independent support comes from the enrichment of the *dg-dh* and *cenH* regions as RNA-DNA hybrids[35]. The Swi6$^{3K\rightarrow3A}$ protein's binding sites may shift from the *dg-dh* repeats to the euchromatin regions because of low affinity promiscuous RNA binding property.

Among chromodomain proteins, Chp1 binds to centromeric nc RNA, while Clr4 binding depends on Lys9-Methylated H3[36]. We suggest that Chp1 may also bind more strongly to ncRNA-DNA hybrid than to ncRNA. Because of evolutionary conservation, the metazoan orthologs of Swi6/HP1 may effect heterchromatinization of centromeric repeats by similar mechanism.

Methods

Strains and plasmids

The strains used in this study are listed in Table 5.

The *rnh1* gene (RNase H1SPBC.336.06c) cDNA was amplified by PCR from genomic DNA and ligated between the *Xho*I and *Bam*HI sites in pREP3X vector to obtain a thiamine repressible *rnh1* expression construct. Similarly, the other construct *nmt1-rnh201* (a gift of J-I. Nakayama[34]), encoding the subunit A of the three subunit enzyme RNase H2 (SPAC4G9.02), was PCR amplified from genomic DNA and cloned between the restriction sites *Bam*HI and *Sal*I upstream of the *nmt1* promoter in the vector pREP1. All fission yeast media were prepared according to Moreno *et.al*.[27]

Genetic Techniques

Sporulation was checked either microscopically or by staining the colonies with iodine vapours. Efficiently switching strains produce equal number of cells of opposite mating type, which mate to form zygotic asci that sporulate on minimal media. The spore cell wall contains a starchy compound that stains dark purple with iodine vapours. Thus, efficiently switching cells of an h^{90} strain grow into colonies that stain dark purple with iodine while colonies of cells that switch inefficiently give light yellowish staining[27]. Determining the percentage of dark colonies provided a semi-quantitative measure of the switching efficiency. After iodine staining the colonies were photographed under Olympus StereoZoom Microscope.

Silencing status of any reporter gene was assessed by monitoring its expression using different plate assays. Expression of the *ura4* reporter was detected by dilution spotting, wherein 5µl of ten-fold serial dilutions of the overnight cultures of the required strains were spotted on non- selective plates, plates lacking urcail and those containing 5'FOA. FOA provided counte-r selection to *ura*$^-$ cells. Thus, ura$^+$ strains that grow well on ura minus but grow poorly on FOA plates, while ura- cells grow poorly on ura minus but grow well on FOA plates. Cell densities of all the cultures were normalized before serial dilution.

Expression of heterochromatic *ade6* was assessed by streaking the cells for single colonies on plates containing limited adenine. Cells expressing *ade6* produced light pink or white colonies on these plates and cells failing to express *ade6* gene produced dark red colonies. The fraction of colonies giving pink/white colour provide a qualitative measure of the silencing defect. Similarly, the extent of silencing of the *his3* locus at subtelomeric locus (*his3-telo*)[28] was measured qualitatively by growth on plates lacking histidine.

Cloning, site-directed mutagenesis, protein over-expression and purification

Lysine residues (KKK) at positions 242-244 in Swi6 were mutated to alanine (AAA) in the *nmt1-GFP-swi6*$^{+}$ expression construct (kindly gifted by Dr. Alison Pidoux) using the QuickChange site-directed mutagenesis kit (Stratagene), as per the manufacturer's instructiaonnds, confirmed by sequencing. The mutant is referred to as *swi6*$^{3K\rightarrow 3A}$. The wild type full length Swi6 and Swi6$^{3K\rightarrow 3A}$ were tagged with GST at amino-terminus by cloning into pGEX-KG expression vector as BamHI-HindIII fragments.

Expression and purification of GST-tagged Swi6 protein

The recombinant constructs containing GST, GST-Swi6, GST-Swi6$^{3K\rightarrow 3A}$, GST-Swi6 -CD, GST-Swi6-CD-Hinge and GST-Swi6 (CSD) were transformed in to BL21(DE3) host cells. The transformed cells were cultured in the LB-Amp medium at 37°C. At mid-log phase, cells were induced with 1mM IPTG and incubated further at 25°C for 8hrs. For purification of GST-tagged proteins, 2-4 mg protein extract was added to 50 µl of Glutathione Sepharose beads (Cat. no. 17527901, GE healthcare Ltd.) equilibrated with 1XPBS and incubated for 10-14 hours at 4°C. Purified proteins were collected after subjecting the mixture to elution for 2hrs at 4°C with 250 µl elution buffer containing 10mM reduced glutathione. Purification was confirmed by SDS- PAGE.

Expression of the *nmt1* promoter driven GFP tagged *swi6*$^{+}$ as well as *swi6*$^{3K\rightarrow -3A}$ gene was induced by removing thiamine from the medium of an overnight grown culture by washing the cells thoroughly and growing them further in medium lacking thiamine. It took 17-18 hrs of induction to achieve maximum expression level. Swi6 protein was detected by Western blotting with either anti-Swi6 (in-house, 1:10000), anti-GFP [Santa Cruz (sc-9996) 1:1000] or anti-GST [Santa Cruz (sc-138), 1:1000] antibodies. Wherever required, anti-a-tubulin antibody (Sigma, cat# T-9026; 1:4000) was used to probe the loading control. Alkaline phosphatase conjugated anti-rabbit (Sigma, cat# A-3562; 1:20,000) antibody was used, as per instructions. Western blots were developed using nitroblue tetrazolium (NBT) and bromo-chloro-indolyl phosphate (BCIP) as chromogenic substrates.

Fluorescence Microscopy

10ml cultures of cells expressing vector, *nmt1-GFP-swi6*$^{+}$ or *nmt1-GFP-swi6*$^{3K\rightarrow -3A}$ in *swi6Δ* background were harvested by centrifugation at 5000 rpm at RT. Cells were fixed in chilled 70% ethanol, rehydrated sequentially in 50%, 30%, 20% ethanol and finally in water. The pellets were resuspended in 50µl of 1X PBS. 5µl of this suspension was then visualized unfldueorrescence microscope. Similar method was

followed for visualizing subcellular localization of chromosomally GFP-tagged Swi6 under the influence of over-expressed *rnh1* and *rnh201*.

Generation of [g-P32] labelled single stranded *in vitro* transcribed RNAs (ssRNA)

a) *In vitro* transcription

For synthesizing the single stranded RNA complementary to the heterochromatin-specific DNA sequences[18,19], an *in vitro* transcription protocol was adapted from Wilusz lab protocol (http:// csu-cvmbs.colostate.edu/academics/mip/wilusz-lab/Pages/lab-protocols.aspx) with suitable modifications. The reaction was carried outby assembling nucleasefree water, 1µl of DNA template (1µg/ µl conc.), 4 µl of ribonucleotidesmix (2.5mM each of ATP, GTP, CTP, and UTP) to a final concentration of 0.5mM, 2 µl of 10X RNA polymerase bufferand 1 µl of T7 RNA polymerase enzyme (Cat. no. AM2178, Ambion) were mixed and dilutedto 20 µl with nuclease- free water and incubatedat 37˚C for exactly 3 hour.s The reaction was subjected to Phenol (pH 5.2)/Chloroform extraction, followed by ethanol precipitation.

b) Polyacrylamide gel elution of *in vitro* transcribed RNAs

To obtain around 500 ng of *in vitro* transcribed RNA, about 10 reactions were set up and pooled. The pellet obtained after precipitation was resuspendedin 20 µl 1X formamide dye and loaded on 10% to 20% acrylamide/8M urea gels depending on the size of the required *in vitro* transcribed RNA. Subsequently, the gel was stained with Syber gold nucleic acid stain (Cat. no. S11494, Invitrogen Life technologies) for visualization under UV transilluminator. The RNA bands were located along the RNA marker (Cat. no. AM7778, Ambion) were excised and frozen at -20 ˚C for 20 min. Thereafter, the gel pieces were crushedand resuspended in 1 ml of Crush and Soak buffer. The tubes were incubated at 37˚C and 700 rpm for 12-14 hrs on a thermo mixer. The supernatant was then subjected to ethanol precipitation.

c) Dephosphorylation of 5’ends of RNA

The ssRNA generated by *in vitro* transcription was dephosphorylated before labeling. The dephosphorylation reaction was set up with 500ng of ssRNA, Alkaline phosphatase calf intestinal enzyme, CIP (Cat. no. M0290, New England BioLabs Inc., USA), 1X CIP buffer, RNase inhibitor (Cat. no. AM2696, Ambion) and nuclease-free water upto 25 µl. The reaction was incubated at 37˚C for 1 hour, phenol/chloroform extracted and ethanol precipitated.

d) 5-end labeling of RNA

To perform 5’-end labeling of dephosphorylated RNA, a reaction mix containing 500ng of dephosphorylated RNA, T4 Polynucleotide kinase (PNK) enzyme (Cat. no. M0201S, New England BioLabs Inc., USA), 1X T4 PNK buffer, RNase inhibitor, [g-^{32}P]-dATP (>3300 Ci/ mmol) was obtained from Board of Radiation and Isotope Technology (BARC), Mumbai and nuclease-free water up to 50ml was prepared

and incubated at 37˚C for 1hr. Unincorporated isotope was removed by passing through microspin G-50 columns (Cat. no. GE27-5330-01, GE Healthcare Ltd.). The eluent was stored at -70˚C and used for performing RNA-EMSA.

e) RNA-DNA hybrid formation

For producing RNA-DNA hybrids, the ssRNA was annealed with equimolar amount of complementary DNA oligo in presence of 1X transcription buffer. The reacting was incubated at 85^{o}C for 5 minutes to remove the secondary structures and was subjected to gradual cooling to 55^{o}C. At 55^{o}C, the reaction was incubated overnight for annealing and checked on 10% native TBE gel before using for the EMSA experiments.

f) Synthesis of long RNAs

For *in vitro* synthesis of 'Revcen' RNA, a long centromeric sequence shown in Djupedal *et al*[19] was PCR amplified and cloned in the Litmus-28i plasmid. The clone containing the DNA sequence complementary to '*RevCen'* RNA was digested with *Hin*dIII to obtain a linear plasmid. The linearized plasmid was used as a template for *in vitro* transcription as described earlier. The reaction containing *in vitro* transcribed RNA was gel purified and subjected to alkaline phosphatase treatment followed by 5'end-labeling with [γ-^{32}P] dATP (10 mCi/µl, specific activity 3300 Ci/mmol) and used for EMSA experiments. The 'Cen100' transcript, as reported by Keller *et al* (SPAC15E1.04)[6], was also synthesized and labeled by the same protocol. The radio-labelled oligonucleotides were purified by passing through a BioGel P-6 column (Biorad Inc.).

Electrophoretic mobility shift assay (EMSA)

For EMSA, purified protein extract was mixed with ss siRNA or siRNA-DNA hybrid that was radiolabeled with [g-^{32}P]ATP with polynucleotide kinase in the binding buffer containing 20mM HEPES (pH 7.5), 50mM KCl, 2mM EDTA, 0.01% NP40, 1mM DTT, 5 units RNase inhibitor, 1 µg BSA and 5% glycerol alongwith ~5 µg budding yeast total RNA or poly dI-dC as non- specific competitor, respectively), followed by incubation on ice. The samples were loaded on native TGE/ polyacrylamide (the tracking dyes Bromophenol blue and Xylene cyanol were not used in loading buffer as they interfere with the binding of proteins with nucleic acids). A negative control (without protein) was also loaded on the gel. 5X loading buffer containing both tracking dyes was added to negative control to track migration. For competition analysis, 0.1, 1.0 and 10 pmol of RNAs and DNAs were used. The gel was dried in gel dryer and exposed to X-ray film scanned in a phosphoimager.

The band intensities of the DNA-protein complex and free DNA for each lane were quantified using Scion Image software and the data were plotted according to a non-linear regression equation corresponding to one site specific-binding model as follows:

Y = Bmax.X /(Kd+X), where Y represents the amount of protein-bound radioactivity, X, the protein concentration, Bmax –the total change in radioactivity counts and Kd, the equilibtium binding constant[23].

Chromatin Immunoprecipitation (ChIP) Assay

Cells of appropriate strains were grown to an OD600 of 0.6 and crosslinked for 30 min with 3% formaldehyde at 18^{o}C. Immunoprecipitation was performed with the following antibodies: 1 µl anti-H3K9me2 (Upstate, 07-353) and 2 µl polyclonal anti-Swi6 per 400 µl reaction. Multiplex radioactive PCR amplifications of the immunoprecipitated chromatin samples, in the presence of α-P^{32}ATP as the source of radiolabelled ATP in addition to non-radioactive dNTPs, were done using the following primers

ADE6F: 5'-TGCGATGCACCTGACCAGGAAAGT-3';

ADE6R: 5'-AGAGTTGGGTGTTGATTTCGCTGA-3'

URA4F: 5'-GAGGGGATGAAAAATCCCAT-3'

URA4R: 5'-TTCGACAACAGGATTACGACC-3'

HIS3F: 5'-AGGTGTCCTTCTTGATGCCA-3'

HIS3R: 5'-CGAATTCCTGCTAGACCGAA-3'

dh For: 5'-GGAGTTGCGCAAACGAAGTT-3'

dh Rev: 5'-CTCACTCAAGTCCAATCGCA-3'

act1F: 5'-TCCTACGTTGGTGATGAAGC-3'

act1R: 5'-TCCGATAGTGATAACTTGAC-3'

The products are resolved on 4% 1X TBE polyacrylamide gel, exposed to magnetic screen and scanned in Fuji ImageProcessor. The bands are quantified densitometrically from three independent sets of PCR using inbuilt MultiGauge Software. Data presented as mean SE. Data was analyzed through one-way ANOVA with Turkey's post-hoc test where *** denotes $p<0.001$ when compared with vector and ns stands for non-significant.

RIP-Seq Analysis

Small RNA was isolated from immunoprecipitated samples from cells expressing GFP-Swi6^{+}, GFP-Swi6$^{3K\rightarrow3A}$ and TAP-Tas3. Cells from 500 ml cultures were harvested at log-phase (OD595= 0.5-0.7) were washed once with 10 ml ice-cold water and once with ice-cold STOP buffer (0.5% SDS, 5mM EDTA pH 8, 100 µg proteinase K) at 4°C. Cells were resuspended in (one-fifth the culture volume) HB buffer (25mM MOPS pH 7.2, 15mM MgCl2, 15mM EGTA, 1mM DTT, 1% Triton-X100, 10% glycerol) supplemented with

PMSF (to a final concentration of 1mM) and protease inhibitor cocktail (PIC) (at 1:100 dilution) and dispensed as 1 ml aliquots into bead beater tubes. Ice-cold zirconium or acid-washed RNase-free glass beads were added upto 500µl mark, given 10-12 pulses of 1 min each alternated with 5 min incubations on ice. The lysate was centrifuged at 13500 rpm at 4°C for 1 hr. The clarified supernatants were removed to fresh tubes and mixed with 100% glycerol to a final concentration of 10%. The expression of the protein of interest can be checked at this point by Western analysis (as described previously).

The extracts were kept at -80°C until further use. For immunoprecipitating TAP tagged proteins, commercially available TAP antibody conjugated agarose beads (Santa Cruz, sc-32319 AC) were used and no coupling was needed. These beads were directly used after equilibration with IP buffer. 2µl of anti-Swi6 antibody was conjugated to 50 µl protein-A sepharose beads (Sigma, P9424-1ml) in a 500 µl 1X PBS containing coupling reaction for 16hrs at 4°C with continuous mixing. The antibody bound beads are then washed twice with 500µl of 0.2M borate buffer (pH 9) and subsequently incubated in 500µl of 0.2M respective borate buffer containing dimethylpimelimidate (DMP) at a concentration of 5mg/ml for 30 minutes at RT with mixing.

DMP-mediated coupling was stopped by washing the beads once with 500µl 0.2M of ethanoleamine (pH 8.0). The residual DMP was quenched by incubating the beads in 500µl 0.2M of ethanoleamine (pH 8.0) for 2 hrs at RT. The beads were then washed once with 1X IP buffer [50mM Tris-Cl (pH 7.5), 150mM NaCl, 0.5% NP40 and 0.5mg/ml BSA). Approximately 3 mg of crude extract was bound in the presence of 1X IP buffer for 16hrs at 4°C with mixing. Beads were then washed once with IP wash buffer [50mM Tris-Cl (pH 7.5), 150mM NaCl, 0.1% NP40 (or 0.1% Tween-20) and 1mM EDTA (pH 8.0)]. To each 50 µl beads loaded with immunoprecipitate, 200µl each of LETS buffer [100mM LiCl, 10mM EDTA (pH8.0), 10mM Tris (pH 7.4), 0.2% SDS] and phenol (pH 5.2) were added. Samples were vortexed gently with intermittent ice incubation (30 sec on, 30sec off) followed by 1 hr at 37°C. The beads are then centrifuged at RT for 5min at 12000rpm. The collected supernatants were extracted once with equal volumes (~400µl) of phenol (pH 5.2): chloroform (1:1). RNA in the upper aqueous phase was precipitated with 20µg glycogen, one-tenth volume of 5M LiCl (40µl) and 2.5 volume of chilled absolute ethanol (1100µl) at -80^{o}C for 16hrs. Pellet was washed with 300µl chilled 80% ethanol and dissolved in 250µl of RNase-free water. To the dissolved RNA, 250µl PEG precipitation solution (20% PEG (MW8000) in 2M NaCl) was added. Contents were incubated on ice for 30 min and centrifuged at 12000rpm for 20 min at 4oC. The supernatants were transferred to fresh tubes while the pellets were first dissolved in TE (pH 8.0), ethanol precipitated, washed with 80% ethanol, dried and resuspended in RNase-free water. This contains the population of long RNA while the supernatant isolated after PEG precipitation contains the small RNAs. Supernatant obtained after PEG precipitation was extracted once with phenol (pH 5.2): chloroform and small RNA present in the aqueous layer was precipitated using LiCl-ethanol system as earlier. The isolated small RNA was checked by running on a 15% 7M denaturing urea gel. This RNA was subjected to Northern blotting with probes complementary to *dh* sequences of the *S. pombe* centromeric repeat regions. Alternatively, they were used as riboprobes for Southern blots of PCR products generated from the

centromeres and the mating type loci of fission yeast, like, *dh, dhk* and *dg*; *act1* was taken as a negative control. Finally, one set of the isolate RNA was subjected to next generation sequencing.

The NEBNext® Multiplex Small RNA Library Prep Set for Illumina based system was used for 3' adaptor ligation, cDNA synthesis, 5' adaptor ligation and PCR, followed by size selection and sequencing using the Illumina platform was performed by Bionivid Technology Pvt. Ltd., Bangalore.

The sequencing data was analyzed using bowtie2 and R-packages as detailed in the following section.

RIP-seq data processing

Gene annotations and reference genome of fission yeast were downloaded from https://www.pombase.org/. Reference genome was indexed using 'bowtie2-build' *

http://bowtie-bio.sourceforge.net/bowtie2/index.shtml). We trimmed the 5' and 3' Illumina small RNA-seq adapters sequences (GUUCAGAGUUCUACAGUCCGACGAUC and TGGAATTCTCGGGTGCCAAGG, respectively) using 'cutadapt' (https://cutadapt.readthedocs.io/). Duplicates were removed using 'rmdup' utility of SeqKit package (https://bioinf.shenwei.me/seqkit). The clean reads were mapped onto the indexed reference genome using bowtie2 with '–sensitive' setting. The quality of the reads was assessed using FastQC (https://www.bioinformatics.babraham.ac.uk/projects/fastqc/) at each step. We binned the raw reads at 5kb (for boxplot) and 200 bp (for line plot) resolutions and quantile normalized the read counts across samples using the function 'normalize.quantiles' of 'preprocessCore' R-package (https://www.bioconductor.org/packages//2.11/bioc/html/preprocessCore.html). The centromere annotations were obtained from https://www.pombase.org/status/centromeres. The telomeric and sub-telomeric regions were defined as 0-50Kb and 50-100Kb regions from the chromosome ends. The read-counts for $swi6^{+}$ and $swi6^{3K\rightarrow 3A}$ samples were divided by those of control ('vector') sample. We calculated the log2 ratio of read counts of $swi6^{3K\rightarrow 3A}$ to $swi6^{+}$ for plotting purpose. Sequence and annotations for mating-type region were obtained from https://www.ncbi.nlm.nih.gov/nuccore/FP565355.1. The reads were independently mapped onto mating-type sequence following the same procedure as earlier and processed at 200 bp resolution. We further identified the 5kb bins that had at-least one of the sequence motifs known to interact with Swi6 (Table X) using in-house script. P-values were calculated using two-tailed Mann-Whitney U tests on R.

The quality scores of RIP-Seq data is shown in Extended Data Table 6.

ChIP-seq data processing

We downloaded the 'sra' files of the ChIP-seq experiments, such as H3K4me3, H3K36me3, H3K9me2, H3K9me3, RNA PolII and Swi6 from GSE83495. We converted the files to 'fastq' format using 'fastq-dump' of NCBI SRAtoolkit. The reads were then mapped on the indexed genome reference using bowtie2 with default parameters. We converted the 'sam' files into 'bam' files using 'samtools' and 'bam' to 'bed' using 'bedtools' with default parameters. We binned the raw reads at 5kb resolution and labeled bins

appropriately when their coordinates mapped into telomeres, centromeres and mating region. We plotted the density of read counts for the bins with RIP-seq log2 ratio (mutant to wild-type) > +1 or < -1. The p-values were calculated using Mann Whitney U tests.

Gene expression analysis

FPKM values for WT pombe strain were downloaded from GSE104546 and the average gene expression was calculated for each 5kb bin. We plotted the distribution of average gene expression values for the bins with RIP-seq log2 ratio (mutant to wild-type) > +1 or < -1. The p- value was calculated using Mann Whitney U test.

DNA-RNA hybrid Immunoprecipitation (DRIP) Analysis

Cells harvested from 500 ml log phase culture were washed with 1X PBS, resuspended in 2 ml PEMS (100mM PIPES, 1mM MgCl2, 1mM EDTA, 1.2 M sorbitol) supplemented with 20ul lyticase/zymolase and keep at 37°C for 30 min for spheroplasting. Spheroplasts were resuspended in 1.6ml TE containing 42ul of 20% SDS and 10ul of 10mg/ml Proteinase K and overnight at 37^{o}C. Supernatant was extracted once with phenol:CIA and genomic DNA in the aqueous phase ethanol precipitated. 10ug of this DNA was digested overnight with Sau3AI at 37°C in 150 µl reaction. Following a phenol clean-up ethanol precipitated Sau3AI digested DNA was dissolved in TE without RNase A. One aliquot of the digested DNA was subjected to overnight RNase H (NEB cat#M0297) treatment at 37°C. Subsequently, RNAse H treated samples were purified through phenol extraction and ethanol precipitation and pellet dissolved in 50 µl TE mixed with binding buffer [10mM NaPO4 (pH 7.0), 0.14M NaCl, 0.05% TritonX-100]. 50 µl of both RNase H treated and untreated samples were saved as non-immunoprecipitated samples (NIPs). The DNA was immunoprecipitated overnight with 2 µl of anti-DNA-RNA hybrid mouse mono clonal antibody[30] (S9.6; ATCC HB8730) at 4°C with constant mixing.

DNA-RNA hybrid/anti-body complex was harvested with protein G Sepharose beads and eluted in a buffer containing 50mM Tris (pH 8.0), 10mM EDTA, 0.5% SDS and 1.5 µg/ml Proteinase K at 55°C for 45 min. DNA from this complex was retrieved through phenol:CIA clean-up followed by ethanol precipitation. 2-3ng of this DNA was used for each RT-qPCR reaction set up with primers specific to the centromeric *dh* repeat region using SYBR Master Mix (ThernoFisher) in QuantStudio3 (ThermoFisher). Fold enrichment was calculated using ΔΔCt method[39].

Declarations

Acknowledgements

The project was supported by extramural funding by the Department of Biotechnology, New Delhi, India and Department of Science and Technology, New Delhi, India and intramural funding by Council of Scientific nd Industrial Research, New Delhi, India. K.R.C was supported by UGC fellowship. We thank Nupur Malhotra for initial observations.

Author contributions

The project was visualized by J.S. and executed primarily by J.K., S.H. and N.G. J.K. and N.G. did most of the EMSA experiments, J.K and S.H. did the silencing assays. S.H. planned and carried out the ChIP, RIP and DRIP experiments, V.K. did confocal microscopy to study the effect of overexpression of rnh1and rnh201 on Swi6 localization, M.T., D.G. and D.D. carried out EMSA assay for RNA-DNA hybrid. K.R.C. and K.S.S. carried out the computational analysis of the RIP-Seq data. S.H. wrote the original draft and J.S., S. H., J.K. and N.G. edited, revised and wrote the manuscript.

Competing Interests

The authors declare no competing interests.

References

1. Nakayama, J., Rice, J.C., Strahl, B.D., Allis, C.D. & Grewal, S. I. Role of histone H3 lysine 9 methylation in epigenetic control of heterochromatin assembly. *Science* **292**, 110-113 (2001).
2. Haldar, S., Saini, A., Nanda, J.S., Saini, S. & Singh, J. Role of Swi6/HP1 self- association-mediated recruitment of Clr4/Suv39 in establishment and maintenance of heterochromatin in fission yeast. *.J. Biol. Chem.* **286**, 9308-9320 (2011)
3. Al-Sady, B., Madhani, H.D. & Narlikar, G. J. Division of labor between the chromodomains of HP1 and Suv39 methylase enables coordination of heterochromatin *Mol. Cell.* **51**, 80-91 (2013).
4. Akhtar, A., Zink, D. & Becker, P. Chromodomains are protein-RNA interaction modules. *Nature*. **407**,405-409 (2000).
5. Muchardt, C., Guilleme, M., Seeler, J. S., Trouche, D., Dejean, A. & Yaniv, M. Coordinated methyl and RNA binding is required for heterochromatin localization of mammalian HP1alpha. *EMBO Rep.* **3**, 975-981 (2002).
6. Keller, C., Adaixo, R., Stunnenberg, R., Woolcock, K. J., Hiller, S. & Bühler, M. HP1(Swi6) mediates the recognition and destruction of heterochromatic RNA *Mol. Cell.* **47**, 215-227 (2012).
7. Volpe, T. A., Kidner, C., Hall, I. M., Teng, G., Grewal, S. I. & Martienssen, R. A. Regulation of heterochromatic silencing and histone H3 lysine-9 methylation by RNAi. *Science*. **297**, 1833-1837 (2002).
8. Jenuwein, T. & Allis, C.D. Translating the histone code. *Science*. **293**, 1074-1080 (2001).
9. Grewal, S. I & Jia, S. Heterochromatin Revisited. *Genet.* **8**, 35-46 (2007)
10. Bannister, A. J., Zegerman, P., Partridge, J. F., Miska, E. A., Thomas, J.O., Allshire, C, & Kouzarides, T. Selective recognition of methylated lysine 9 on histone H3 by the HP1 chromo domain. *Nature.* **410**, 120-124 (2001).
11. Canzio D, Chang EY, Shankar S, Kuchenbecker KM, Simon MD, Madhani HD, Narlikar GJ, Al-Sady B. Chromodomain-mediated oligomerization of HP1 suggests a nucleosome-bridging mechanism for

heterochromatin assembly. *Mol. Cell*. **41**, 67-81 (2011).

12. Holoch, D. & Moazed, D. Small-RNA loading licenses Argonaute for assembly into a transcriptional silencing complex. *Struct. Mol. Biol.* **22**, 328-35 (2015).
13. Verdel, A., Jia, S., Gerber, S., Sugiyama, T., Gygi, S., Grewal, S.I. & Moazed. D. RNAi- mediated targeting of heterochromatin by the RITS complex. **303**, 672-676 (2004).
14. Sugiyama, T., Cam, H., Verdel, A., Moazed, D. & Grewal, S.I. RNA-dependent RNA polymerase is an essential component of a self-enforcing loop coupling heterochromatin assembly to siRNA production. *Natl. Acad. Sci. U.S.A.* **102**, 152-157 (2005).
15. Martienssen, & Moazed, D. RNAi and Heterochromatin Assembly. *Cold Spring Harb. Perspect. Biol*. **7**, a019323 (2015).
16. , E.H., White, S.A., Kagansky, A., Bijos, D. A., Sanchez-Pulido, L., Hoe, K. L., Kim, D. U, Park, H. O, Ponting, C. P, Rappsilber, J, Allshire RC.Stc1: a critical link between RNAi and chromatin modification required for heterochromatin integrity. *Cell*. **140**, 666-677 (2010).
17. Hong, E-J., Villén,, Gerace, E. L., Gygi, S. P. & Moazed, D. A Cullin E3 Ubiquitin Ligase Complex Associates With Rik1 and the Clr4 Histone H3-K9 Methyltransferase and Is Required for RNAi-mediated Heterochromatin Formation. *RNA Biol.* **2**, 106-111 (2005).
18. Reinhart, B. J. & Bartel, D. P. Small RNAs correspond to centromere heterochromatic *Science*. **297**, 1831 (2002).
19. Djupedal, I., Kos-Braun, I. C., Mosher, R. A., Söderholm, N., Simmer, F., Hardcastle, T. J., Fender, A., Heidrich, N., Kagansky, A., Bayne, E., Wagner, E. G., Baulcombe, D. C., Allshire, R. C. & Ekwall, K. Analysis of small RNA in fission yeast; centromeric siRNAs are potentially generated through a structured RNA. *EMBO J.* **28**, 3832-3844 (2009).
20. Grewal, S. I. & Klar, A. J. A recombinationally repressed region between mat2 and mat3 loci shares homology to centromeric repeats and regulates directionality of mating-type switching in fission yeast. *Genetics*. **146**,1221-1238 (1997).
21. Hansen, K. R., Ibarra, P. T. & Thon, G. Evolutionary-conserved telomere-linked helicase genes of fission yeast are repressed by silencing factors, RNAi components and the telomere-binding protein Taz1. *Nucleic Acids Res*. **34**, 78-88 (2006).
22. Bailey, T. L., Boden, M., Buske A., Frith, M., Grant, C. E., Clementi, L., Jingyuan Ren, J., Li, W. W., & Noble, W.S. MEME SUITE: tools for motif discovery and searching. *Nucleic Acids Res.* 37(Web Server issue): W202–W208 (2009).
23. Heffler, M. A., Walters, R.D. & Kugel, J. F. Using electrophoretic mobility shift assays to measure equilibrium dissociation constants: GAL4-p53 binding DNA as a model system. *Mol, Biol. Educ.* **40**, 383-387 (2012).
24. Kanoh, J., Sadaie, M., Urano, T. & Ishikawa, F. Telomere binding protein Taz1 establishes Swi6 heterochromatin independently of RNAi at telomeres. *Biol.* **15**, 1808-1819 (2005).
25. Pidoux, A.L., Uzawa, S., Perry, P. E., Cande, W. Z. & Allshire, R. C. Live analysis of lagging chromosomes during anaphase and their effect on spindle elongation rate in fission yeast. *Cell. Sci.*

113, 4177-4191 (2000).

26. Allshire, R. C., Javerzat, J-P., Redhead, N. J. & Cranston, G. Position effect variegation at fission yeast centromeres. *Cell* **76**, 157-169 (1994)
27. Moreno,, Klar, A. & Nurse, P. Molecular Genetic Analysis of Fission Yeast Schizosaccharomyces pombe. *Methods Enzymol.***194**,795-823 (1991).
28. Cooper, J. P., Nimmo, E. R., Allshire, R. C. & Cech, T. R. Regulation of telomere length and function by a Myb-domain protein in fission yeast. *Nature*. **385**, 744-747 (1997).
29. Ginno, P. A.,Lott, P.L., Christensen. H. C., Korf, I. & Chedin, F. R-loop formation is a distinctive characteristic of unmethylated human CpG island promoters. *Cell.* **45**, 977-986 (2012).
30. Boguslawski, S. J., .Smith, D. E., Michalak, A., Mickelson, K. E., Yehle, C. O., Patterson, W. L. & Carrico, R. J. Characterization of monoclonal antibody to DNA · RNA and its application to immunodetection of hybrids. J. Imm. Methods. **89**, 123-130 (1986)
31. Wang, W., Stevenson, A. L., Kearsey,S. E., Watt, S. & Bähler, J. Global Role for Polyadenylation-Assisted Nuclear RNA Degradation in Posttranscriptional Gene Silencing. *Mol. Cell. Biol.* **28**, 656-65 (2008).
32. Morris, S. A., Shibata, Y., Noma, K-I., Tsukamoto, Y., Warren, E., Temple, B., Grewal,
33. I. S. & Strahl, B. D. Histone H3 K36 methylation is associated with transcription elongation in *Schizosaccharomyces pombe*. *Eukaryotic Cell*. **4**, 1446-1454 (2005)
34. Shimada, Y., Mohn, F., & Bühler, M. The RNA-induced transcriptional silencing complex targets chromatin exclusively via interacting with nascent transcripts *Genes Dev*. **30**, 2571-2580 (2016).
35. Nakama, M., Kawakami, K., Kajitani, T., Urano, T. & Murakami, Y. DNA-RNA hybrid formation mediates RNAi-directed heterochromatin formation. *Genes Cells*. **17**, 218-233.
36. Dutrow, N., Nix, D. A., Holt, D.,Milash, B., Dalley, B., Westbroek, E., Parnell, T. J. & Cairns, B. R. Dynamic transcriptome of *Schizosaccharomyces pombe* shown by RNA-DNA hybrid mapping. *Nat. Genet.* **40**, 977–986 (2008).
37. Ishida, M., Shimojo, H., Hayashi, A., Kawaguchi, R., Ohtani, Y., Uegaki, K., Nishimura,
38. & Nakayama, J. Intrinsic nucleic acid-binding activity of Chp1 chromodomain is required for heterochromatic gene silencing. *Mol. Cell.* **47**, 228-241 (2012).
39. Thon, G., Cohen, A. & Klar, A. Three Additional Linkage Groups That Repress Transcription and Meiotic Recombination in the Mating-Type Region of Schizosaccharomyces Pombe. *Genetics* **138**, 29-38 (1994)
40. Thon, G., Bjerling, K. P. & Nielsen, I. S. Localization and Properties of a Silencing Element Near the mat3-M Mating-Type Cassette of Schizosaccharomyces pombe. *Genetics* **151**, 945-963 (1999).
41. Livak, K. J. & Schmittgen, T. D. Analysis of Relative Gene Expression Data Using Real- Time Quantitative PCR and the 22DDC T Method. *Methods* **25**, 402–408 (2001)

Figures

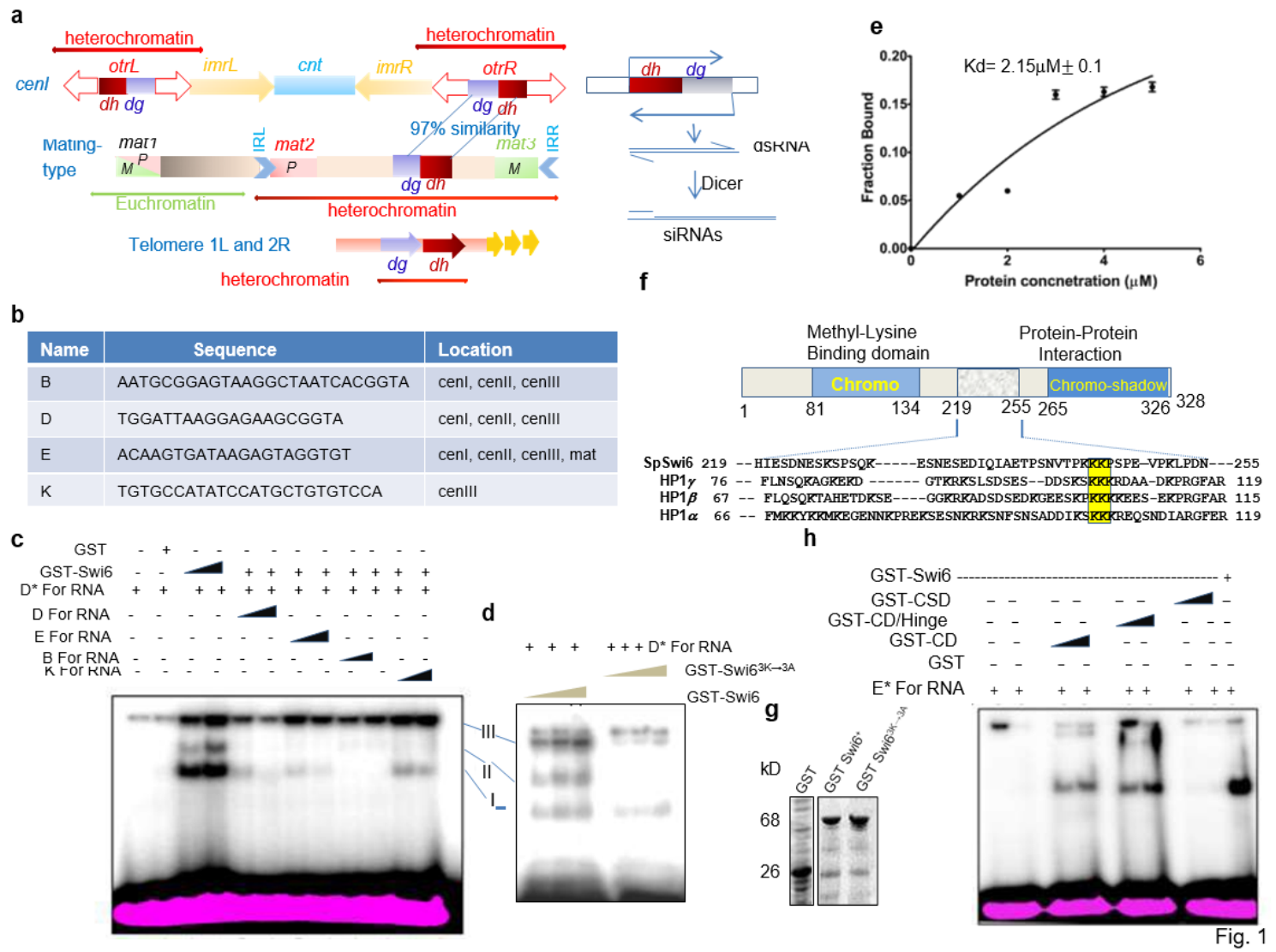

Fig. 1

Figure 1

Sequence-specific binding of Swi6 to the dg.dh specific siRNAs in vitro. a, Schematic representation of the dg and dh regions in the centromere, mating type (cenH) and the subtelomeric genes. tlh1 and tlh2. Right panel, a schematic showing siRNAs being generated from the dg-dh sequences. b, List of si RNA sequences, reported by Reinhardt and Bartel18, that were synthesized in vitro. c, EMSA assay showing sequence specific binding of Swi6 to the ss D-For RNA and its competition by excess col RNA sequences B,D, E and K. Arrows indicate the complexes I, II and II between Swi6 and 'D-For' RNA. d, The mutant Swi63K→3A shows weaker binding to the D-For RNA. EMSA was performed as in c. e, Estimation of equilibrium binding constant (Kd) for the binding of Swi6 to D-For RNA. The data of protein concentration of Swi6 along X axis and the fraction of siRNA bound was plotted according to Ref. 23. f, Schematic depiction of the domain structure of Swi6 showing the chromo-, chromo-hinge and chromoshadow domains. Alignment of the sequences of the hinge domain between HP1□, HP1□, HP1□ and Swi6, showing conservation of the lysine triplet located at residues 242-244. g, SDS- PAGE showing the purified GST, GST-Swi6 and GST-Swi63K→3A. h, EMSA showing that the RNA binding could be ascribed primarily to the CD and CD-hinge but not the CSD.

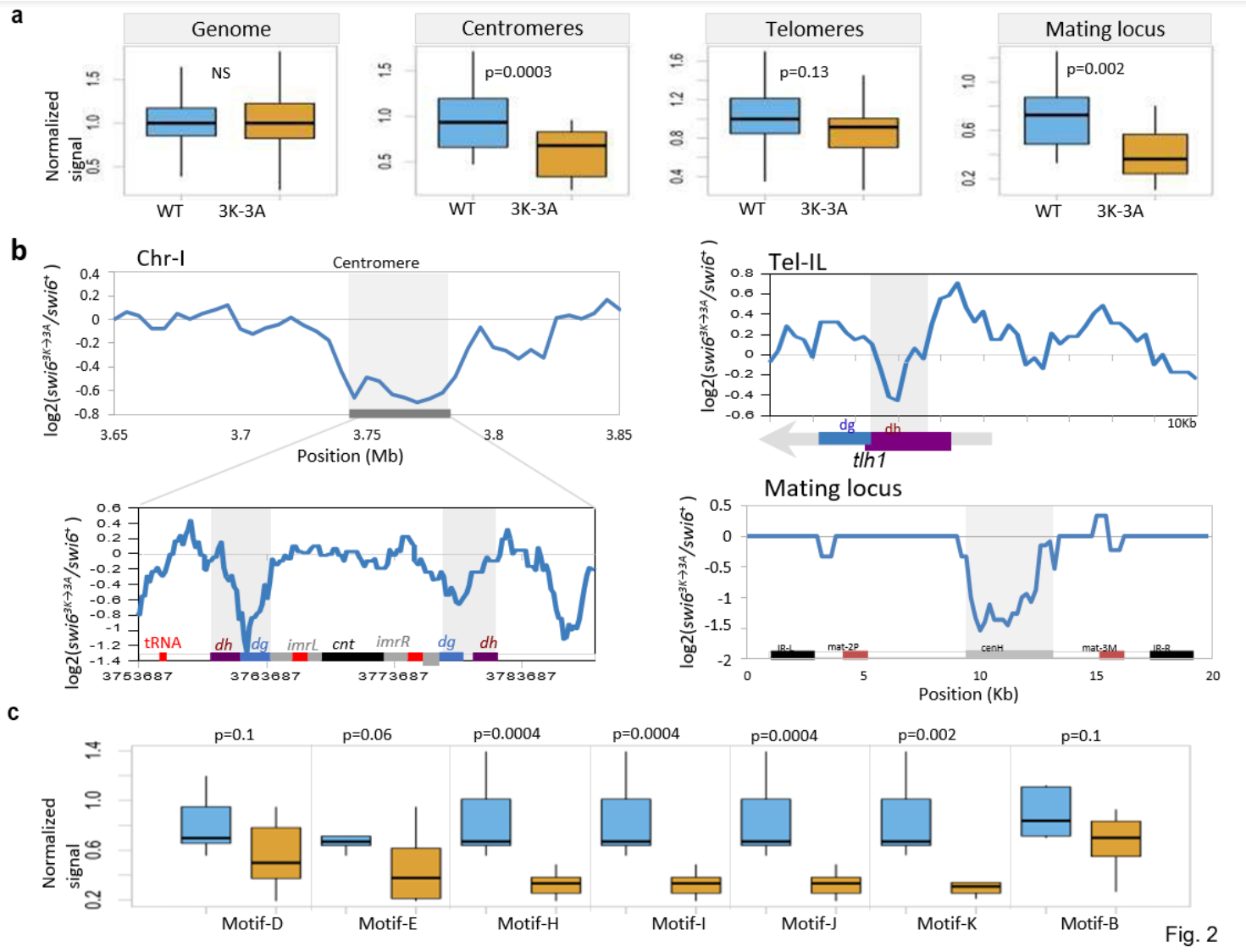

Fig. 2

Figure 2

Localization of Swi6-bound siRNAs to dg-dh regions is abrogated in swi63K→3A mutant. a, Overall distribution of normalized small-RNA accumulation at centromeres, telomeres and mating-type locus in WT and swi63K→3A mutant. b, Chromosomal track of RIP-seq fold change (log2 3K-3A/WT ratio) at and around centromere of chr-I at 5kb (top) and 200bp (bottom) resolutions, left telomere of chr-I (200bp resolution) and the mating locus (200bp resolution). Locus annotations are given at the bottom of the plot. Plots for other centromeres and telomeres are given in the Extended Data, Fig. 8. c, Distributions of normalized RIP-seq signals in swi6+ and swi63K→3A strains for regions containing the sequence motif(s) known to interact with Swi6. The p-values were calculated using two-tailed Mann-Whitney U tests.

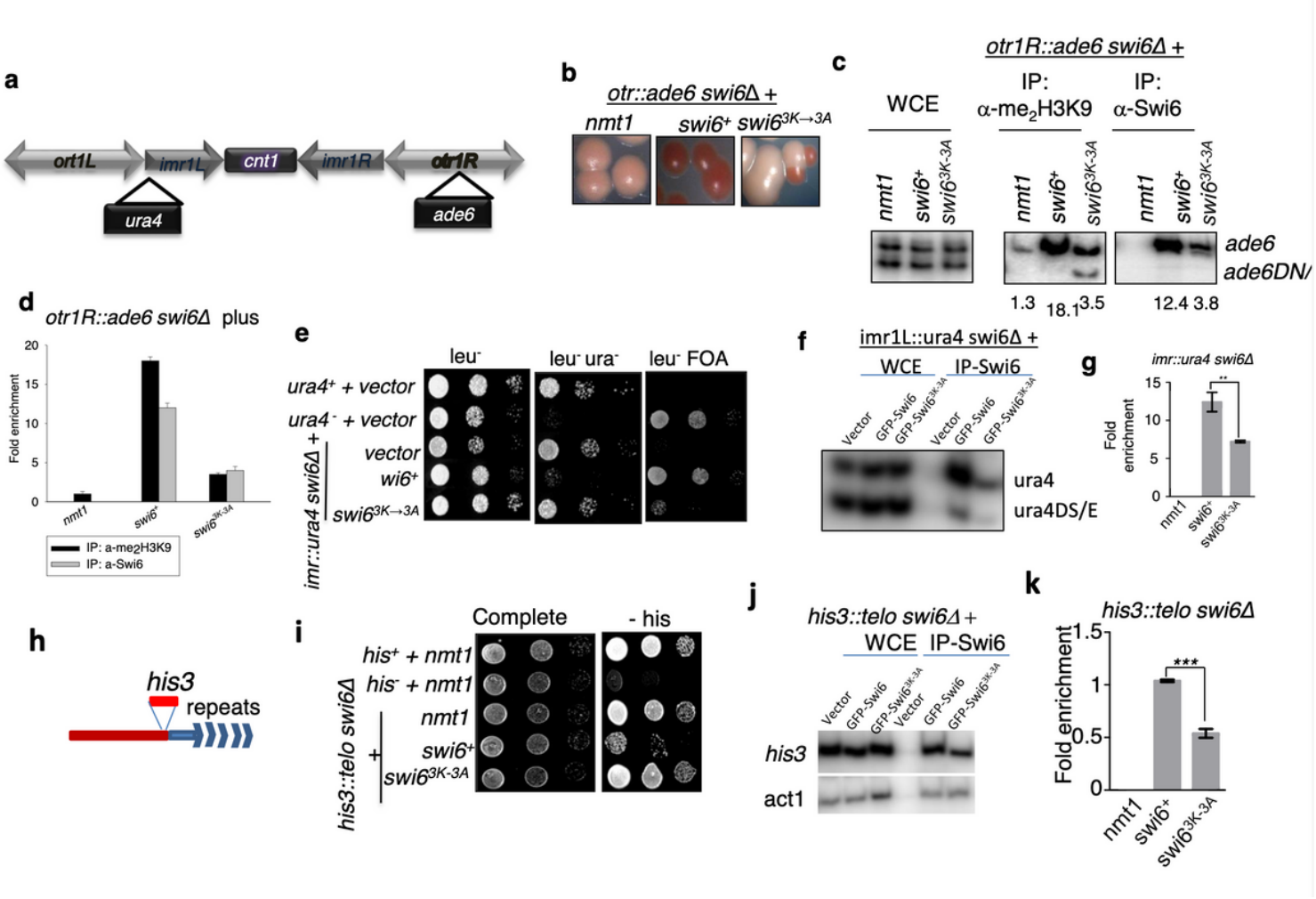

Figure 3

Abrogation of silencing in swi63K→3A mutant accompanies Swi6 delocalization at the outer repeat otr1R and imr1L regions of cenI and his3-telo. a, Diagrammatic representation of the genotype of the strain. Centromere of each fission yeast chromosome comprises of a central core (cnt), immediately flanked on both sides by inverted repeats (imr); imr on either side are flanked by outer repeat regions (otr). Reporter genes ura4, ade6 and his3 have been inserted into the imr, otr of centromere and telomeric repeats, respectively of chrI. The strain has a swi6Δ mutation and carries internal deletions in native ura4 locus, denoted as ura4DS/E, and in ade6, denoted as ade6DN/N, which act as euchromatic controls in ChIP assay. b-d Derepression of the otr1R::ade6 locus in swi63K→3A mutant, showing pink/white colonies on adenine limiting plates (b). c, ChIP assay showing reduction of Me2-K9-H3 and Swi6 at the ade6 locus in swi63K→3A mutant. Ratio of the heterochromatic ade6 and euchromatic ade6DN/N locus is shown d. Quantitation of data shown in c. e, Spotting assay showing inability of swi63K→3A to restore silencing at the imr1::ura4 locus in swi6 mutant, as indicated by growth on plates lacking uracil and lack of growth on FOA plates. f, ChIP assay showing delocalization of Swi6 from the imr1::ura4 locus in the swi63K→3A mutant, where ura4 represents the heterochromatin and ura4DS/E the euchromatin. g, Quantitation of the data showing enrichment of Swi6 at ura4 versus ura4DS/E in f. h-k, Derepression of the subtelomeric his3 locus in swi63K→3A mutant. h, gives a schematic representation of the his3 gene inserted distal to

the telomeric repeats, denoted as his3-telo28. i, Spotting assay showing the enhanced growth of the strain having his3-telo reporter in presence of the swi63K→3A mutation on plates lacking histidine. j, ChIP assay reduced localization of mutant Swi63K→3A at the his3-telo locus as compared to wt. act1 was used as a control. k, Quantitation of data shown in j.

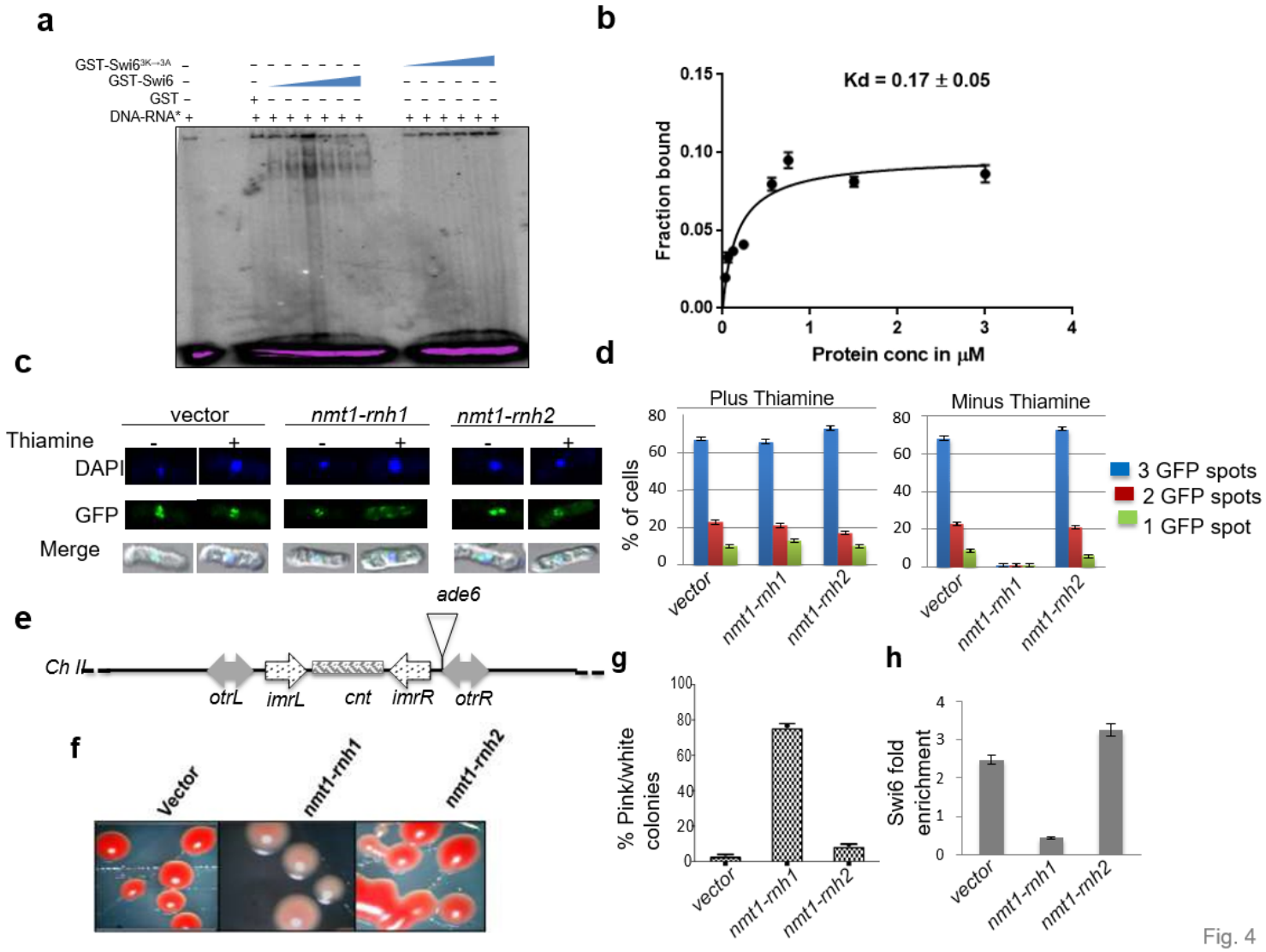

Fig. 4

Figure 4

Role of Swi6 binding to the dg.dh sequences as RNA-DNA hybrids in silencing. a, Swi6 shows strong affinity towards the RNA-DNA hybrid. EMSA assay was performed using the hybrid between the D-For RNA and its complementary DNA sequence and purified GST- Swi6 or GST-Swi63K→3A. GST was used as control. b, Data in a was plotted according to Ref. 23 to determine the equilibrium binding constant, Kd. c, Fluorescence micrographs showing the effect of overexpressed nmt1-rnh1 and nmt1-rnh201 on the subcellular localization of Swi6 with respect to the three heterochromatic loci, mat, cen and tel as distinct green foci. The strain had the native copy of swi6 gene chromosomally tagged with GFP. Nuclei were stained with DAPI. d, Microscopic data has been quantified as distinct green foci pertaining to GFP-Swi6 subcellular localizing to the heterochromatic loci. e, Schematic representation of the gen centromere II having an ade6 reporter gene inserted into the otr1R. f, The effect of over-expressed vector alone (nmt1),

nmt1-GFP-swi6 or nmt1-GFP-swi63K→3A on the expression of the ade6 reporter was evaluated by streaking on adenine limiting plates. Colors of the colonies indicated the state of the ade6 reporter. Red colonies indicate suppression of ade6 repression while pint/white colonies indicated repression. g, This observation is represented in terms of percent white colonies. h, Depression of ade6 reporter at otr1R repeat as a result of overexpression of swi6+ or swi63K→3A as observed in g was biochemically verified through Swi6 enrichment at the locus through ChIP assay. Delocalization of GFP-Swi6 upon overexpression of rnh1 but not rnh201. c, Confocal microscopy. Strains expressing GFP-tagged Swi6 was transformed with vector alone, rnh1 or rnh201 under the control of nmt1 promoter. Transformed cells were grown in the presence (+) or absence (-) of the repressor, thiamine, visualized under confocal microscope and photographed. d, Quantitation of the localization of GFP-Swi6 as three, two or one spots. e, Overexpression of rnh1 causes loss of silencing at the otr1R::ade6 locus. The transformed cells of the strain having otr1R::ade6 locus were grown on plates containing limiting adenine. After growth on selective plates for 4-5 days at 30oC, the colonies were photographed. g, Plot showing the per cent colonies giving pink/white appearance in different transformants, as shown in f. h, Delocalization of Swi6 from the otr1R::ade6 locus in the transformants shown in f.